Twin-Field Quantum Key Distribution with Local Frequency Reference

Jiu-Peng Chen,[1,2] Fei Zhou,[1,2] Chi Zhang,[1,2] Cong Jiang,[1,2] Fa-Xi Chen,[1,2] Jia Huang,[3] Hao Li,[3] Li-Xing You,[3] Xiang-Bin Wang,[1,2,4] Yang Liu,[1,2] Qiang Zhang,[1,2,5] and Jian-Wei Pan[2,5]

[1]*Jinan Institute of Quantum Technology and CAS Center for Excellence in Quantum Information and Quantum Physics, University of Science and Technology of China, Jinan 250101, China*

[2]*Hefei National Laboratory, University of Science and Technology of China, Hefei 230088, China*

[3]*State Key Laboratory of Functional Materials for Informatics, Shanghai Institute of Microsystem and Information Technology, Chinese Academy of Sciences, Shanghai 200050, China*

[4]*State Key Laboratory of Low Dimensional Quantum Physics, Department of Physics, Tsinghua University, Beijing 100084, China*

[5]*Hefei National Research Center for Physical Sciences at the Microscale and School of Physical Sciences, University of Science and Technology of China, Hefei 230026, China*

(Received 20 October 2023; accepted 21 May 2024; published 28 June 2024)

Twin-field quantum key distribution (TFQKD) overcomes the linear rate-loss limit, which promises a boost of secure key rate over long distance. However, the complexity of eliminating the frequency differences between the independent laser sources hinders its practical application. We analyzed and determined the frequency stability requirements for implementing TFQKD using frequency-stabilized lasers. Based on this analysis, we proposed and demonstrated a simple and practical approach that utilizes the saturated absorption spectroscopy of acetylene as an absolute reference, eliminating the need for fast frequency locking to achieve TFQKD. Adopting the 4-intensity sending-or-not-sending TFQKD protocol, we experimentally demonstrated the TFQKD over 502, 301, and 201 km ultralow-loss optical fiber, respectively. We expect this high-performance scheme will find widespread usage in future intercity and free-space quantum communication networks.

DOI: 10.1103/PhysRevLett.132.260802

Introduction.—Quantum key distribution (QKD) [1–6] offers an information-theoretically secure way to share secure keys between distant users. Since the quantum signal is forbidden to be amplified [7] and decays exponentially with the transmission distance, without a quantum repeater, the point-to-point secret key capacity scales linearly with the channel transmission [8], which poses an inevitable barrier for long-distance QKD. As an efficient version of measurement-device-independent (MDI) QKD [9,10], the twin-field QKD (TFQKD) [11] improves the secure key rate to overcome the linear rate-loss limit [8], which enhances the key rate to the square root scale of the channel transmittance with current available technologies. Therefore, the combination of measurement-device independence and excellent tolerance on channel loss made TFQKD rapidly becoming the focus of competing research once it was proposed. At present, TFQKD has obtained many achievements in theory [11–15] and experiment [16–30]. These efforts pave the way for the realization of long-distance quantum communication networks with enhanced security and improved performance.

However, implementing TFQKD is challenging, because the protocols require coherently controlling the twin light fields from remote parties. Any phase differences caused by frequency differences between independent lasers or channel fiber fluctuations may disturb the coherence of the twin light fields. Currently, the phase differences caused by hundreds of kilometers of fiber fluctuations are generally limited and can be effectively compensated using mature techniques, either in real time [17,23,25,28] or through postprocessing methods [18,20–22,24,26,30]. The fast phase variations originating from the light sources without frequency locking can be much more severe than that caused by long fiber fluctuations. By fast frequency locking such as time-frequency metrology [18,20,24,26–28,30] or the optical phase locking loop [16,17,23,25], the relative frequency differences are real-time eliminated with gigantic and complicated settings on light sources. Alternatively, through the high-speed single-photon detection and the fast Fourier transform (FFT) algorithm [29], the relative frequency differences could be eliminated in postprocessing with high-count measurement devices and complex data postprocessing operations in a measurement station. All these previous methods could potentially hinder its wide application.

Moreover, the scarcity of free-space link channels means that an additional channel for frequency locking [16–18,20,23–28,30] could increase the cost and complexity of free-space TFQKD. Meanwhile, generating secure keys on small data sizes is inevitable in free-space experiments due to their weather dependence; therefore, data postprocessing operations [29] could impede efficient data collection during implementation of TFQKD in free space.

Here, we analyzed the relative phase drift between separate lasers that are hundreds of kilometers apart and determined that frequency-stabilized lasers, demonstrating typical absolute frequency stability with an Allen deviation [31–33] better than 1×10^{-10}, are capable of fulfilling the requirements for implementing TFQKD. Based on this criterion, we proposed the utilization the technique of saturated absorption spectroscopy of acetylene as a replacement for the previous methods employed to eliminate the relative frequency differences between lasers. This approach leverages the two acetylene cells as absolute frequency standards, enabling the stabilization of the frequency drift of Alice's and Bob's seed fiber lasers with a stability better than 2×10^{-12}, respectively. As a result, the frequency differences between light sources are effectively constrained to vary within a narrow range of less than 300 Hz. With the implementation of these two stabilized light sources, we demonstrated the 4-intensity sending-or-not-sending (SNS) TFQKD [13] with the actively-odd-parity-pairing [34–37] method over different fiber lengths. Our approach simplifies the system by eliminating the need for a shared optical frequency reference and an additional fiber channel for laser locking between lasers, without increasing the complexity of measurement devices or data postprocessing. Furthermore, without servo-induced noise on rapidly frequency locking on laser sources, a high-performance single-photon interference to support a low phase flip error rate of less than 3% is obtained; thus, the final secure key rates corresponding to total sent pulses as few as 2×10^{11} are still considerable. In other words, if the similar system frequency of about 1 GHz to that in Refs. [25,30] is used, a considerable secure key rate can be obtained at the minutes level.

In the promotion of the practical application of quantum communication, which overcomes the linear rate-loss limit, there are two related works [28,38] that demonstrate different approaches by applying the so-called mode-pairing protocol. Without relative frequency locking between independent laser sources, Refs. [28,38] simplify the setup compared to previous demonstrations on TFQKD. Nonetheless, the final secure key rate of the mode-pairing protocol depends entirely on the postselecting time slots within the coherence time of the laser sources. As a result, without ultrastable laser sources that have a much longer coherence time but add more complexity and cost [28], the final secure key rate and tolerable transmission loss are lower than those of TFQKD.

The experimental setup is shown in Fig. 1(a). Alice and Bob use two continuous wave (cw) fiber lasers with a linewidth of several hundred hertz which are referenced to

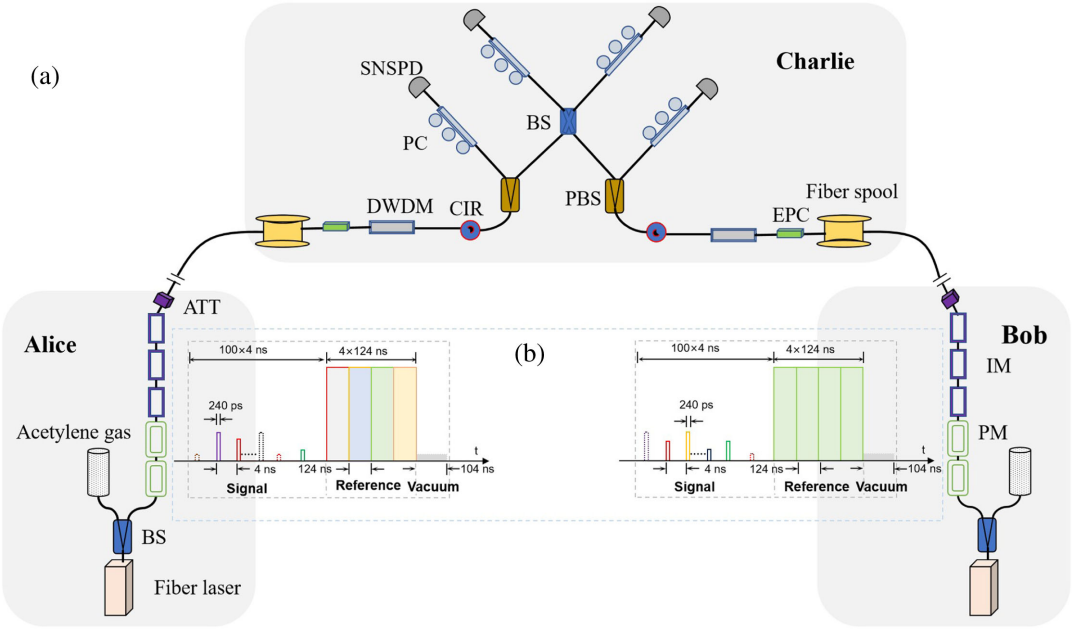

FIG. 1. (a) Schematic of experimental setup. In Alice's and Bob's lab, two acetylene-stabilized lasers are employed as the light sources. These lasers are then modulated with two phase modulators (PMs) and three intensity modulators (IMs) to generate a waveform pattern that time multiplexes the weak signal pulses with strong phase reference pulses and attenuates them to bring the signal pulses to the single-photon level with an attenuator (ATT). The prepared light pulses are finally sent to Charlie through the ultralow-loss fiber spools for detection. Charlie uses a dense wavelength division multiplexer (DWDM) and a circulator (CIR) to filter the noises before the polarization beam splitter (PBS) and the beam splitter (BS). The interference results are detected by superconducting nanowire single-photon detectors (SNSPDs). EPC, electric polarization controller; PC, polarization controller. (b) Waveform pattern of the modulation. The cw light beam is modulated to a waveform pattern that 100 signal pulses are time multiplexed with four strong phase reference pulses in a basic period.

the saturated absorption spectroscopy of acetylene [39,40] as their light sources. The narrow linewidth cw light beam, with a central wavelength of 1542.3837 nm, is then modulated to generate a waveform pattern [as shown in Fig. 1(b)] where the single-photon-level quantum signal pulses are time multiplexed with strong phase reference pulses. The generated light pulses are transmitted to Charlie through ultralow-loss (ULL) fiber spools. Upon reaching Charlie's beam splitter (BS), they interfere, and the resulting signals are detected by two superconducting nanowire single-photon detectors (SNSPDs) before being recorded by a time tagger.

Crucially, the realization of TFQKD involves controlling the phase evolution of the fields, which travel hundreds of kilometers through the channel before interfering at Charlie's BS. The fast relative phase drift rate between the two optical fields sent from users hundreds of kilometers apart to Charlie can be written as

$$\frac{d(\Delta\Phi)}{dt} = 2\pi\left[\frac{\sqrt{2}\bar{\nu}}{S}\frac{\partial\bar{l}}{\partial t} + \frac{\sqrt{2}\bar{l}}{S}\frac{\partial\bar{\nu}}{\partial t} + (\nu_1 - \nu_2) + \sqrt{2}t\frac{\partial\bar{\nu}}{\partial t}\right], \quad (1)$$

where $\Delta\Phi$ is the differential phase between the two optical fields, ν_1 and ν_2 are the output frequency of the lasers, S is the light speed in the fiber, $\bar{\nu} = (\nu_1 + \nu_2/2)$, $\bar{l} = (l_1 + l_2/2)$, l_1 and l_2 are the fiber lengths, and t is the time slot during relative phase detection. The first term in Eq. (1) represents long fiber fluctuation, while the second and fourth terms are related to the lasers' short-term linewidth and fast frequency drift. The second term indicates rapid phase variation caused by the lasers' fast frequency drift during the interval of laser transmission over long fiber links, while the fourth term shows rapid phase variation caused by the lasers' fast frequency drift during the interval of relative phase detection. The third term represents fast relative phase fluctuations caused by frequency differences between lasers, which is related to the slow frequency drift and long-term stability of the lasers' frequency. Numerical calculations reveal that the fast relative phase variation related to short-term linewidth and fast frequency drift can be ignored. It is much smaller than the phase variation caused by long fiber fluctuation and frequency differences between the lasers. Moreover, improving the long-term stability and eliminating gradual frequency drift to achieve an absolute frequency stability better than 1×10^{-10} in laser frequency stabilization is capable of fulfilling the requirements for implementing TFQKD. (See Supplemental Material for details of the laser frequency stabilization requirements for implementing TFQKD using independent lasers [41,42].)

In C-band optical communication, gas-based absorption spectroscopy, such as hydrogen cyanide (HCN) and acetylene, is commonly employed to stabilize laser frequency, thereby improving long-term stability and eliminating gradual frequency drift. However, differences in the structure and properties of molecules and atoms, as well as external factors such as temperature, pressure, and gas purity, could impact the accuracy and stability of these methods. As a result, not all gas-based absorption spectroscopy methods can meet the requirements. For example, HCN gas-based absorption spectroscopy in free-space MDIQKD achieves a frequency stability of approximately 1×10^{-7} [43], which falls short of the requirements for TFQKD. In contrast, acetylene's specific transitions offer more precise and well-defined frequencies with a stability better than 2×10^{-12} [39,40], making it a good choice for implementing TFQKD (see Supplemental Material [41] for details of the acetylene-stabilized laser). By referring to the acetylene cells, as shown in Fig. 2(a), the frequency differences between the two independent fiber lasers are restricted to slow variation within a small range of 300 Hz. Under the influence of the frequency differences, as shown in Fig. 2(b), the phase fluctuation rate of the two independent light sources is about 0.015 rad/μs [here, it is important to note that, in order to effectively measure phase variations on the order of microseconds (μs), the acquisition bandwidth of the interference signal must be set much higher than 1 MHz; however, this increase in bandwidth can introduce high-frequency electronic noise, which may cause the measured phase drift to appear faster than its actual value], which is comparable to the fluctuation of hundreds of kilometers of fiber links in the

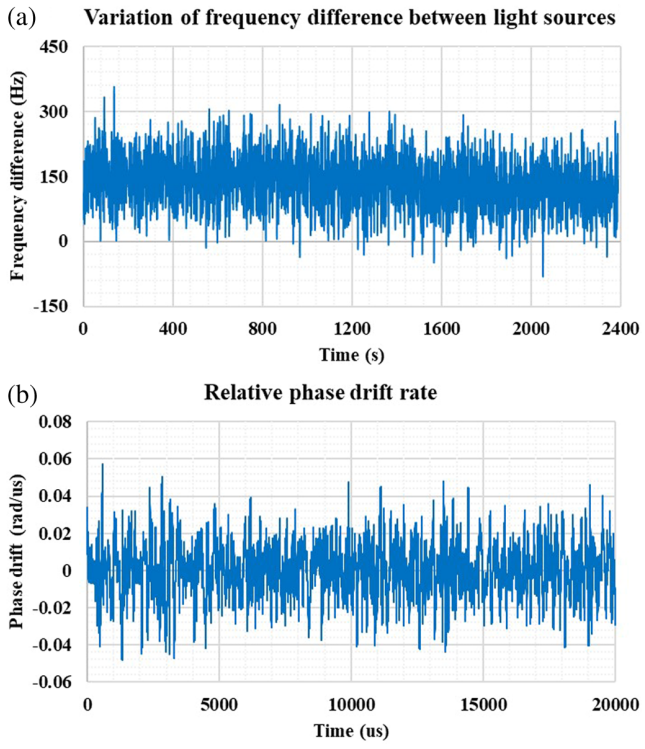

FIG. 2. (a) Variation of the frequency difference between the light sources. (b) Relative phase drift rate between the light sources.

field [24] and can be eliminated through fiber fluctuation suppression.

After configuring the light sources, the emitted cw light beams from them are encoded to generate a waveform pattern that 100 signal pulses are time multiplexed with four strong phase reference pulses within a basic period. For each basic period of 1 μs time sequence, 100 signal pulses with four random intensities and 16 random phase values are prepared in the first 400 ns, each with a 240 ps pulse duration and 3.76 ns interval. Then four strong phase reference pulses with the same intensity and fixed phase values are prepared in the following 496 ns, each with a 124 ns pulse duration. Finally, an extinction pulse with a duration of 104 ns is prepared to recover the SNSPDs before starting a new transmission period. Before the prepared pulses are sent out of Alice's and Bob's labs, they are attenuated on both sides to bring the signal pulses to the single-photon level with passive attenuators. Through two symmetrical fiber links consisting of ultralow-loss fiber spools, the two pulse trains arrive at Charlie and interfere at a BS. The interference results are detected by two SNSPDs and recorded by a high-speed multichannel time tagger.

To suppress system noise, two dense wavelength division multiplexers operating at the central wavelength of 1548.15 nm with a bandwidth of 100 GHz are inserted in Charlie to filter the nonlinear scattering light that originates from the strong phase reference pulses [20]. Additionally, two circulators are inserted to prevent the strong reference pulses from being reflected off the end face of the SNSPDs into the optical fiber links, thus scattering backward noise [20].

To ensure that the twin-field light pulses arrive at Charlie's BS with identical polarization and timing, feedback devices are incorporated to adjust the channel delay and polarization. Before the twin-field light pulses from Alice and Bob interfere at Charlie's BS, a polarization beam splitter (PBS) is inserted. Real-time monitoring of the idle beam of the PBS allows for the detection of changes in polarization and channel delay caused by fluctuations in the fiber paths. An electric polarization controller is then employed to adjust the polarization accordingly. Additionally, the clock phase of the encoding signal sources is adjusted approximately every 20 s to compensate for variations in channel delay.

In addition to polarization and arrival time perturbations, fluctuations in fiber paths can also introduce disturbances in the global phase of the signal pulses. However, these disturbances were effectively eliminated through the application of the postdata selection method [18].

After considering all of the above, we performed symmetrical 4-intensity SNS TFQKD over various lengths of ULL optical fibers: 201, 301, and 502 km. The total losses, including connections, were 33.6, 50.4, and 83.7 dB, with an average of 0.167 dB/km. The total insertion loss of the optical components was optimized to 1.8 dB in Charlie. Then, we adopted two high-performance SNSPDs with a detection efficiency of 70% and 72%, along with an effective dark count rate of 0.2 Hz for both, to detect the interference results. We set a time gate of 0.3 ns to suppress noise, resulting in an additional loss of 1.2 dB. To get high key rates, we applied the advanced decoy-state analysis method in the decoy-state analysis and the advanced key distillation scheme to extract the final keys (see Supplemental Material [41] for details of the protocol). Taking into account the finite data size effect [34,44], we then calculated the secure key rates [37].

As shown in Fig. 3, the obtained secure key rates were $R = 8.74 \times 10^{-5}$, $R = 1.15 \times 10^{-5}$, and $R = 9.67 \times 10^{-8}$ for the three different distances, respectively (see Supplemental Material [41] for details of the experimental results). Here, we emphasize that, although our key rate is similar to that of several recent works [27–29,38], our system is less complex and more cost effective. Reference [27] used ultrastable lasers and electro-optic frequency combs for the phase reconciliation of the twin fields. Reference [29] employed high-count measurement devices and a fast FFT algorithm for the same purpose. References [28,38] demonstrated results using the mode-pairing protocol.

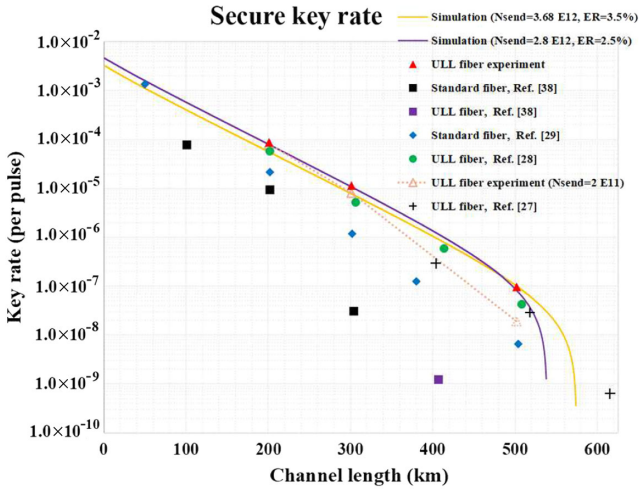

FIG. 3. Secure key rates of the SNS TFQKD experiment. The red triangles indicate the experimental results over 201 km, 301 km ULL fiber with a total sent pulses of 2.87×10^{12}, and 502 km ULL fiber with a total sent pulses of 3.68×10^{12}; the brown triangles indicate the experimental results while the total sent pulses are curtailed to a small size of 2×10^{11}. The black cross represents the experimental results from Ref. [27]. The green dot and purple square represent the experimental results from Refs. [28,38], respectively, obtained over the ULL fiber. Meanwhile, the black square and blue diamond indicate the experimental results from Refs. [29,38], respectively, over the standard fiber. The purple curve is the simulation result with our experimental parameters that a total of 2.87×10^{12} pulses are sent and the phase flip error rate is 2.5%. The orange curve shows the simulation result with our experimental parameters that a total of 3.68×10^{12} pulses are sent and the phase flip error rate is 3.5%.

In conclusion, we have analyzed the phase drift between separate lasers and determined that frequency-stabilized stability better than 1×10^{-10} can fulfill the requirements for implementing TFQKD. Based on this criterion, we proposed a practical approach to implement TFQKD using local optical oscillators referenced to the saturation absorption of acetylene. Subsequently, we experimentally demonstrated TFQKD over different lengths of ULL fibers. Compared to previous works, our approach may have limitations in terms of wavelength selection flexibility and potential challenges in channel multiplexing when used in conjunction with classical optical communication, as it relies on the frequency of the gas-based absorption spectrum. Nonetheless, our Letter offers an effective and practical solution for TFQKD, taking a significant step toward various applications, especially in free-space scenarios with limited channel resources and weather-dependent implementation. Furthermore, our approach eliminates the need for a shared optical frequency reference and an extra fiber channel for laser locking between lasers, improving scalability, cost effectiveness, and robustness. This is particularly advantageous for large networks that no longer require a uniform optical frequency reference.

This work was supported by the Key R&D Plan of Shandong Province (Grants No. 2021ZDPT01, No. 2023CXPT105, and No. 2020CXGC010105), the National Key Research and Development (R&D) Plan of China (Grant No. 2020YFA0309800), the Innovation Program for Quantum Science and Technology (2021ZD0300700), the National Natural Science Foundation of China (Grants No. T2125010, No. 12374470, and No. 12174215), the Chinese Academy of Sciences, Shandong provincial natural science foundation (Grants No. ZR2022LLZ011, No. ZR2023LLZ007, and No. ZR2021LLZ005). Y. L. and Q. Z. acknowledge support from the Taishan Scholar Program of Shandong Province. Q. Z. was supported by the XPLORER prize from New Corner Stone Science Foundation.

J.-P. C., F. Z., and C. Z. contributed equally to this work.

[1] Charles H. Bennett and Gilles Brassard, Quantum cryptography: Public key distribution and coin tossing, in *Proceedings of IEEE International Conference on Computers, Systems and Signal Processing, Bangalore, India* (IEEE, New York, 1984), pp. 175–179.

[2] Nicolas Gisin, Grégoire Ribordy, Wolfgang Tittel, and Hugo Zbinden, Quantum cryptography, Rev. Mod. Phys. **74**, 145 (2002).

[3] Nicolas Gisin and Rob Thew, Quantum communication, Nat. Photonics **1**, 165 (2007).

[4] Valerio Scarani, Helle Bechmann-Pasquinucci, Nicolas J Cerf, Miloslav Dušek, Norbert Lütkenhaus, and Momtchil Peev, The security of practical quantum key distribution, Rev. Mod. Phys. **81**, 1301 (2009).

[5] Feihu Xu, Xiongfeng Ma, Qiang Zhang, Hoi-Kwong Lo, and Jian-Wei Pan, Secure quantum key distribution with realistic devices, Rev. Mod. Phys. **92**, 025002 (2020).

[6] Stefano Pirandola, Ulrik L. Andersen, Leonardo Banchi, Mario Berta, Darius Bunandar, Roger Colbeck, Dirk Englund, Tobias Gehring, Cosmo Lupo, Carlo Ottaviani *et al.*, Advances in quantum cryptography, Adv. Opt. Photonics **12**, 1012 (2020).

[7] W. K. Wootters and W. H. Zurek, A single quantum cannot be cloned, Nature (London) **299**, 802 (1982).

[8] Stefano Pirandola, Riccardo Laurenza, Carlo Ottaviani, and Leonardo Banchi, Fundamental limits of repeaterless quantum communications, Nat. Commun. **8**, 15043 (2017).

[9] Hoi-Kwong Lo, Marcos Curty, and Bing Qi, Measurement-device-independent quantum key distribution, Phys. Rev. Lett. **108**, 130503 (2012).

[10] Samuel L Braunstein and Stefano Pirandola, Side-channel-free quantum key distribution, Phys. Rev. Lett. **108**, 130502 (2012).

[11] Marco Lucamarini, Zhiliang L. Yuan, James F. Dynes, and Andrew J. Shields, Overcoming the rate–distance limit of quantum key distribution without quantum repeaters, Nature (London) **557**, 400 (2018).

[12] Xiongfeng Ma, Pei Zeng, and Hongyi Zhou, Phase-matching quantum key distribution, Phys. Rev. X **8**, 031043 (2018).

[13] Xiang-Bin Wang, Zong-Wen Yu, and Xiao-Long Hu, Twin-field quantum key distribution with large misalignment error, Phys. Rev. A **98**, 062323 (2018).

[14] Marcos Curty, Koji Azuma, and Hoi-Kwong Lo, Simple security proof of twin-field type quantum key distribution protocol, npj Quantum Inf. **5**, 64 (2019).

[15] Feng-Yu Lu, Zhen-Qiang Yin, Chao-Han Cui, Guan-Jie Fan-Yuan, Rong Wang, Shuang Wang, Wei Chen, De-Yong He, Wei Huang, Bing-Jie Xu, Guang-Can Guo, and Zheng-Fu Han, Improving the performance of twin-field quantum key distribution, Phys. Rev. A **100**, 022306 (2019).

[16] M. Minder, M. Pittaluga, G. Roberts, M. Lucamarini, J. Dynes, Z. Yuan, and A. Shields, Experimental quantum key distribution beyond the repeaterless secret key capacity, Nat. Photonics **13**, 334 (2019).

[17] Shuang Wang, De-Yong He, Zhen-Qiang Yin, Feng-Yu Lu, Chao-Han Cui, Wei Chen, Zheng Zhou, Guang-Can Guo, and Zheng-Fu Han, Beating the fundamental rate-distance limit in a proof-of-principle quantum key distribution system, Phys. Rev. X **9**, 021046 (2019).

[18] Yang Liu, Zong-Wen Yu, Weijun Zhang, Jian-Yu Guan, Jiu-Peng Chen, Chi Zhang, Xiao-Long Hu, Hao Li, Cong Jiang, Jin Lin *et al.*, Experimental twin-field quantum key distribution through sending or not sending, Phys. Rev. Lett. **123**, 100505 (2019).

[19] Xiaoqing Zhong, Jianyong Hu, Marcos Curty, Li Qian, and Hoi-Kwong Lo, Proof-of-principle experimental demonstration of twin-field type quantum key distribution, Phys. Rev. Lett. **123**, 100506 (2019).

[20] Jiu-Peng Chen, Chi Zhang, Yang Liu, Cong Jiang, Weijun Zhang, Xiao-Long Hu, Jian-Yu Guan, Zong-Wen Yu, Hai Xu, Jin Lin *et al.*, Sending-or-not-sending with independent

lasers: Secure twin-field quantum key distribution over 509 km, Phys. Rev. Lett. **124**, 070501 (2020).
[21] Xiao-Tian Fang, Pei Zeng, Hui Liu, Mi Zou, Weijie Wu, Yan-Lin Tang, Ying-Jie Sheng, Yao Xiang, Weijun Zhang, Hao Li *et al.*, Implementation of quantum key distribution surpassing the linear rate-transmittance bound, Nat. Photonics **14**, 422 (2020).
[22] Hui Liu, Cong Jiang, Hao-Tao Zhu, Mi Zou, Zong-Wen Yu, Xiao-Long Hu, Hai Xu, Shizhao Ma, Zhiyong Han, Jiu-Peng Chen *et al.*, Field test of twin-field quantum key distribution through sending-or-not-sending over 428 km, Phys. Rev. Lett. **126**, 250502 (2021).
[23] Mirko Pittaluga, Mariella Minder, Marco Lucamarini, Mirko Sanzaro, Robert I. Woodward, Ming-Jun Li, Zhiliang Yuan, and Andrew J. Shields, 600 km repeater-like quantum communications with dual-band stabilisation, Nat. Photonics **15**, 530 (2021).
[24] Jiu-Peng Chen, Chi Zhang, Yang Liu, Cong Jiang, Wei-Jun Zhang, Zhi-Yong Han, Shi-Zhao Ma, Xiao-Long Hu, Yu-Huai Li, Hui Liu *et al.*, Twin-field quantum key distribution over a 511 km optical fibre linking two distant metropolitan areas, Nat. Photonics **15**, 570 (2021).
[25] Shuang Wang, Zhen-Qiang Yin, De-Yong He, Wei Chen, Rui-Qiang Wang, Peng Ye, Yao Zhou, Guan-Jie Fan-Yuan, Fang-Xiang Wang, Wei Chen, Yong-Gang Zhu, Pavel V. Morozov, Alexander V. Divochiy, Zheng Zhou, Guang-Can Guo, and Zheng-Fu Han, Twin-field quantum key distribution over 830-km fibre, Nat. Photonics **16**, 154 (2022).
[26] Jiu-Peng Chen, Chi Zhang, Yang Liu, Cong Jiang, Dong-Feng Zhao, Wei-Jun Zhang, Fa-Xi Chen, Hao Li, Li-Xing You, Zhen Wang, Yang Chen, Xiang-Bin Wang, Qiang Zhang, and Jian-Wei Pan, Quantum key distribution over 658 km fiber with distributed vibration sensing, Phys. Rev. Lett. **128**, 180502 (2022).
[27] Lai Zhou, Jinping Lin, Yumang Jing, and Zhiliang Yuan, Twin-field quantum key distribution without optical frequency dissemination, Nat. Commun. **14**, 2041 (2023).
[28] Lai Zhou, Jinping Lin, Yuan-Mei Xie, Yu-Shuo Lu, Yumang Jing, Hua-Lei Yin, and Zhiliang Yuan, Experimental quantum communication overcomes the rate-loss limit without global phase tracking, Phys. Rev. Lett. **130**, 250801 (2023).
[29] Wei Li, Likang Zhang, Yichen Lu, Zheng-Ping Li, Cong Jiang, Yang Liu, Jia Huang, Hao Li, Zhen Wang, Xiang-Bin Wang, Qiang Zhang, Lixing You, Feihu Xu, and Jian-Wei Pan, Twin-field quantum key distribution without phase locking, Phys. Rev. Lett. **130**, 250802 (2023).
[30] Yang Liu, Wei-Jun Zhang, Cong Jiang, Jiu-Peng Chen, Chi Zhang, Wen-Xin Pan, Di Ma, Hao Dong, Jia-Min Xiong, Cheng-Jun Zhang, Hao Li, Rui-Chun Wang, Jun Wu, Teng-Yun Chen, Lixing You, Xiang-Bin Wang, Qiang Zhang, and Jian-Wei Pan, Experimental twin-field quantum key distribution over 1000 km fiber distance, Phys. Rev. Lett. **130**, 210801 (2023).
[31] James A. Barnes, Andrew R. Chi, Leonard S. Cutler, Daniel J. Healey, David B. Leeson, Thomas E. McGunigal, James A. Mullen, Warren L. Smith, Richard L. Sydnor, Robert F. C. Vessot *et al.*, Characterization of frequency stability, IEEE Trans. Instrum. Meas. **IM-20**, 105 (1971).
[32] Christian Sanner, Nils Huntemann, Richard Lange, Christian Tamm, Ekkehard Peik, Marianna S. Safronova, and Sergey G. Porsev, Optical clock comparison for Lorentz symmetry testing, Nature (London) **567**, 204 (2019).
[33] Jie Li, Xing-Yang Cui, Zhi-Peng Jia, De-Quan Kong, Hai-Wei Yu, Xian-Qing Zhu, Xiao-Yong Liu, De-Zhong Wang, Xiang Zhang, Xin-Yun Huang *et al.*, A strontium lattice clock with both stability and uncertainty below, Metrologia **61**, 015006 (2024).
[34] Cong Jiang, Zong-Wen Yu, Xiao-Long Hu, and Xiang-Bin Wang, Unconditional security of sending or not sending twin-field quantum key distribution with finite pulses, Phys. Rev. Appl. **12**, 024061 (2019).
[35] Hai Xu, Zong-Wen Yu, Cong Jiang, Xiao-Long Hu, and Xiang-Bin Wang, Sending-or-not-sending twin-field quantum key distribution: Breaking the direct transmission key rate, Phys. Rev. A **101**, 042330 (2020).
[36] Cong Jiang, Xiao-Long Hu, Zong-Wen Yu, and Xiang-Bin Wang, Composable security for practical quantum key distribution with two way classical communication, New J. Phys. **23**, 063038 (2021).
[37] Xiao-Long Hu, Cong Jiang, Zong-Wen Yu, and Xiang-Bin Wang, Universal approach to sending-or-not-sending twin field quantum key distribution, Quantum Sci. Technol. **7**, 045031 (2022).
[38] Hao-Tao Zhu, Yizhi Huang, Hui Liu, Pei Zeng, Mi Zou, Yunqi Dai, Shibiao Tang, Hao Li, Lixing You, Zhen Wang, Yu-Ao Chen, Xiongfeng Ma, Teng-Yun Chen, and Jian-Wei Pan, Experimental mode-pairing measurement-device-independent quantum key distribution without global phase locking, Phys. Rev. Lett. **130**, 030801 (2023).
[39] Jan Hald, Lars Nielsen, Jan C. Petersen, Poul Varming, and Jens E. Pedersen, Fiber laser optical frequency standard at 1.54 μm, Opt. Express **19**, 2052 (2011).
[40] Petr Balling, Marc Fischer, Philipp Kubina, and Ronald Holzwarth, Absolute frequency measurement of wavelength standard at 1542 nm: Acetylene stabilized DFB laser, Opt. Express **13**, 9196 (2005).
[41] See Supplemental Material at http://link.aps.org/supplemental/10.1103/PhysRevLett.132.260802 for detailed theoretical scheme, detailed experimental technologies, and full experimental results, which includes Ref. [42].
[42] W. J. Zhang, X. Y. Yang, H. Li, L. X. You, C. L. Lv, L. Zhang, C. J. Zhang, X. Y. Liu, Z. Wang, and X. M. Xie, Fiber-coupled superconducting nanowire single-photon detectors integrated with a bandpass filter on the fiber end-face, Supercond. Sci. Technol. **31**, 035012 (2018).
[43] Yuan Cao *et al.*, Long-distance free-space measurement-device-independent quantum key distribution, Phys. Rev. Lett. **125**, 260503 (2020).
[44] Cong Jiang, Xiao-Long Hu, Hai Xu, Zong-Wen Yu, and Xiang-Bin Wang, Zigzag approach to higher key rate of sending-or-not-sending twin field quantum key distribution with finite-key effects, New J. Phys. **22**, 053048 (2020).